

Design Analysis of 0.5HP Three-Phase PWM Inverter-fed Induction Motor Circuit.

Ogunyemi, J., Bitrus, I. Fagbuaro, E.

(Department of Electrical/Electronic Engineering, The Federal Polytechnic Ilaro, Ogun State, Nigeria.)

Corresponding Author: Ogunyemi, J.

ABSTRACT: The use of pulse width modulation (PWM) in inverter's applications has become popular over the years. This is because it has a well-designed control strategy which allows control of the output in noiseless and more efficient ways. However, inverter's design often requires the analysis of the main components involved. This paper presents a design analysis of a 0.5hp three-phase induction motor driven by a pulse width modulated (PWM) inverter. The mathematical models for the circuit elements involved are derived analytically. The derivation of line current, circuit elements, switching frequency, harmonic voltage, pulse width and its location for a three-phase modulated inverter were presented using Fourier series analysis. The numerical values for the 0.5hp induction motor obtained are 370Ω , 680mH and 3000Hz for resistance, inductance and switching frequency respectively. The design approach can be employed in other applications.

KEYWORDS: PWM, Inverter, Induction Motor, Switching frequency and Harmonics.

Received 04 Dec., 2022; Revised 14 Dec., 2022; Accepted 16 Dec., 2022 © The author(s) 2022.

Published with open access at www.questjournals.org

I. INTRODUCTION

Pulse Width Modulation (PWM) is a well-designed control strategy which allows control of the output in noiseless and more efficient ways. The ability of the PWM method to control the output and eliminate lower-order harmonics makes it popular [1][2][3]. Applications such as motor speed, electric heater, and variable frequency drive (VFD), are common areas where it is used. Other areas of applications include fan regulators, heating ventilation and air conditioning (HVAC), compressor drives, hybrid electric vehicle motor drive circuits, Light Emitting Diode (LED) dimmers switch, etc. PWM inverter-fed induction motor is now finding application in electric vehicles [4]. The extensive use of PWM schemes in the recent time in various applications such as Variable speed drives (VSDs) and fixed frequency shifters (SFCs) as well as uninterruptible power supplies (UPS) have been well reported[5]. The speed of electric motors used in appliances could be varied with PWM and draws only the rated current of the appliance with no consumption of the unused heat which has a negative effect on the efficiency of the motor.

An inverter configuration involves several topologies of power circuits and ways to control the voltage. The most tedious part of the inverter configuration is the waveform generation and control scheme. Figure1 shows a block diagram of a PWM scheme. [6][7].

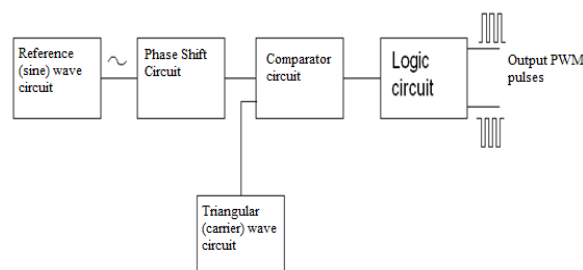


Fig 1: The block diagram of PWM stages[6]

Capacitors and inductors are the major components used for filtering the waveform produced at the output. Low pass filters are used to minimize the harmonics from the output waveform. To obtain high-quality sinusoidal output voltage with reduced harmonics distortion, a multicarrier PWM control scheme is proposed for

a diode clamped multilevel inverter[8]. Resonant filters could also be used if the output frequency of the inverter has a fixed value [9].

An induction motor is an electromechanical machine which generates two magnetic fields; namely: rotor magnetic field and a rotating stator magnetic field. The rotor rotates in such a way that it aligns its magnetic field with that of the stator field. It has a 3-phase set of currents which are equal in magnitude to each other and displaced from 120° from each other. For an inverter-fed induction motor, it is very important to select appropriately the controller and the input waveform[10]. Modern industrial automation is very much dependent on the control of induction motors [11].

The output of an inverter contains harmonics due to the presence of nonlinear elements. Sine wave PWM produces an output voltage waveform which is a pulse-width modulated six-step wave. It contains all the harmonics of the six-step wave with additional high-frequency switching harmonics. The pole voltage waveform has a particularly large harmonic at the carrier frequency because the carrier ratio P is a multiple of three. This carrier harmonic which is a triple harmonic does not appear across the three-phase, three-wire load. The dominant switching harmonics with output voltage are sidebands of twice the carrier frequency, and multiple thereof. Thus, there are major odd harmonic voltage components of the order $k = 2p + 1$, with smaller components of order $2p = 5$ (Note that $2p$ have been suppressed). At high carrier ratios, the harmonic amplitude is practically independent of carrier ratio P. There is a linear relationship between the magnitude of the fundamental voltage and the modulation index [12]. Increased harmonic content increases motor losses in square wave PWM. The advantage of a high carrier ratio in a square wave PWM inverter is that the dominant switching harmonics are at high frequency with resulting current harmonics more readily filtered by the leakage inductance of the motor.

Paper [6] presents a proposed electronics simulation of a phase shift circuit for three-phase pulse width modulated (PWM) inverter. Similarly, the design and implementation of triangular waveform and pulse generators for a three-phase PWM inverter feeding an induction motor were equally presented in [7]. Since the simulation and implementation had been implemented and presented earlier; there is a need to present the mathematical analysis of the PWM inverter presented in those papers.

II. METHODOLOGY

Inverter design often requires the analysis of the main components involved. The mathematical expressions for these elements are derived analytically in this paper. The derivation of line current, circuit elements consisting of resistor and inductor, switching frequency, harmonic equations for three-phase and the pulse width and its location modulated inverter were presented.

1. Derivation of load current

The instantaneous line-line voltage can be expressed in Fourier series with the even harmonics zero as:

$$V_{ab} = \sum_{n=1,3,5,\dots}^{\infty} \frac{4V_s}{n\pi} \cos \frac{n\pi}{6} \sin n(\omega t + \pi/6) \quad \text{----> (1)}$$

$\pi/6$ because V_{ab} is shifted by 30°.

The other two phases can be expressed thus:

$$V_{bc} = \sum_{n=1,3,5,\dots}^{\infty} \frac{4V_s}{n\pi} \cos \frac{n\pi}{6} \sin n(\omega t - \pi/2) \quad \text{----> (2)}$$

$$V_{ca} = \sum_{n=1,3,5,\dots}^{\infty} \frac{4V_s}{n\pi} \cos \frac{n\pi}{6} \sin n(\omega t - 7\pi/6) \quad \text{----> (3)}$$

It can be observed that the triple n harmonics (n= 1, 3, 5...) is zero in line-line voltages.

For a wye-connected load, expression for line current can be obtained from above given impedance Z.

$$Z = \sqrt{R^2 + (n\omega L)^2}$$

The line current i_a for load is therefore given as:

$$i_a = \sum_{n=1,3,5,\dots}^{\infty} \left[\frac{4V_s}{\sqrt{3}n\pi\sqrt{R^2 + (n\omega L)^2}} \cos \frac{n\pi}{6} \right] \sin(n\omega t - \theta_n) \quad \text{----> (4)}$$

Where

$$\theta_n = \tan^{-1} \left(\frac{n\omega L}{R} \right) \quad \text{----> (5)}$$

From equation 5, the instantaneous phase current is given by:

$$i_a = 0.3\sin(314t - 30^\circ) - 0.0225\sin 5(314.2t-71^\circ) - 0.011\sin 7(314.2t-76^\circ) + 0.0049\sin 11(314.2t-84^\circ) + 0.0035\sin 13(314.2t-82^\circ)$$

2. Circuit components sizing

For an induction motor of 0.5HP, the apparent power is 0.375kVA. With power factor of 0.86 lagging; i.e. the phase angle is 30° The real power is $0.375\cos 30 = 0.325\text{kW}$. For each phase, the power is 0.125kVA or 125VA. The phase voltage V_p in a three- phase motor with line voltage of 400V is:

$$V_p = \frac{400}{\sqrt{3}} = 230.9\text{V}$$

Phase current is obtained from:

$$I_p = \frac{125}{230.9} = 0.54\text{A}$$

Impedance Z_L

$$Z_L = \frac{230.9}{0.54} = 427.6\Omega \text{ or } 428\Omega$$

Hence,

$$R = Z\cos\theta = 428\cos 30 = 370\Omega$$

Similarly, for inductance;

$$X_L = Z \sin \theta \text{ or}$$

$$L = \frac{Z \sin \theta}{2\pi f} = \frac{429 \sin 30}{314.2} = 0.68 \text{H or } 680 \text{mH}$$

3. Switching frequency

The next step in the design approach is to find an appropriate value of inverter switching frequency so that the power losses of the inverter at nominal load are minimised. In order to choose a suitable switching frequency, it can be specified that the current waveform is to be stable within 'p' percent. Then the minimum frequency to attain this goal can be computed. The following shows the equivalent circuit of the motor, and the current waveform as the PWM signal switches on and off. This shows the worst case, at 50:50 PWM ratios, and the current rise is shown for a stationary or stalled motor, which is also worst case.

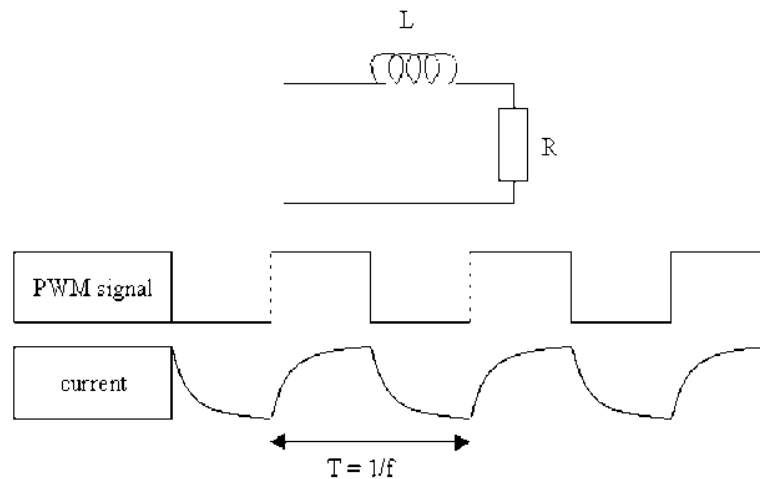


Figure 2: Induction motor equivalent circuit, PWM signal & current waveform [13].

T is the switching period, which is the reciprocal of the switching frequency. Just taking the falling edge of the current waveform, this is given by the equation

$$i = I e^{-\frac{t}{\tau}} = I e^{-\frac{tR}{L}} \text{ ----> (6)}$$

Where τ is the time constant of the circuit, which is L / R .

So the current at time $t = T/2$ (i_1) must be no less than P% lower than at $t = 0$ (i_0). This means there is a limiting condition[13]:

$$i = \left(1 - \frac{P}{100}\right) \cdot i_0 \text{ ----> (7)}$$

$$\Rightarrow I e^{-\frac{TR}{2L}} = \left(1 - \frac{P}{100}\right) I e^0 \quad \text{-----> (8)}$$

$$e^{-\frac{TR}{2L}} = \left(1 - \frac{P}{100}\right) \quad \text{----> (9)}$$

$$T = \frac{-2L}{R} \ln \left(1 - \frac{P}{100}\right) \quad \text{-----> (10)}$$

Since the frequency f is $f = 1/T$

$$\therefore f = \frac{R}{-2L \ln \left(1 - \frac{P}{100}\right)} \quad \text{---->(11)}$$

From equation 11 above, the value of frequency can be determined given the percentage of P.

For P= 10%

$$f = \frac{370}{-2.0.68. \ln \left(1 - \frac{10}{100}\right)}$$

= 2582.2Hz

Therefore, frequency of 3000Hz is chosen.

4. Harmonic Analysis

The total harmonic distortion, THD is

$$THD = \frac{1}{V_1} \left(\sum_{n=2,3,\dots}^{\infty} V_n^2\right)^{1/2} \quad \text{---->(12)}$$

The line-line rms voltage is

$$V_{rms} = \left[\frac{2}{2\pi} \int_0^{2\pi/3} V_s^2 \theta(\omega t)\right]^{1/2} \quad \text{---->(13)}$$

$$= \sqrt{\frac{2}{3}} V_s \quad \text{---->(14)}$$

= 0.8165Vs or 163.3V.

From equation above, the rms nth component of the line voltage is:

$$V_{LN} = \frac{4V_s}{\sqrt{2n\pi}} \cos \frac{n\pi}{6} \quad \text{---->(15)}$$

Which for n=1 gives the fundamental line voltage

$$V_{L1} = \frac{4V_s \cos 30}{\sqrt{2}\pi} \quad \text{----> (16)}$$

= 0.7797Vs or 155.94V

From equation

$$\left(\sum_{n=5,7,11}^{\infty} V_{LN}^2\right)^{1/2} = \left(V_L^2 - V_{LN}^2\right)^{1/2} \quad \text{---->(17)}$$

$$= \sqrt{163.3^2 - 155.94^2} V_s$$

= 48.4%

This value is too high and there is need for harmonic filter its reduction. However, the design of such filter is not presented in this paper.

5. Derivation of pulse width and its location

The general form of a Fourier series for the instantaneous output voltage is

$$V_o(t) = \sum_{n=1,3,5}^{\infty} B_n \sin n\omega t \quad \text{---->(18)}$$

The coefficient B_n in above equation can be determined by considering a pair of pulses such that the positive pulse of duration δ starts at $\omega t = \alpha$ and the negative one of the same width starts at $\omega t = \pi + \alpha$. The effect of all

pulses can be combined together to obtain the effective output voltage. If δ_m is the width of the mth pulse, the

rms output voltage is given as:

$$V_o(t) = V_s \left[\sum_{n=1,3,5}^{\infty} B_n \sin n\omega t \right]^{1/2} \quad \text{---->(19)}$$

if the pulse of mth pair start at $\omega t = \alpha_m$ and ends at $\omega t = \pi + \alpha_m$, the Fourier coefficient for a pair of pulses is

$$B_n = \frac{1}{\pi} \left[\int_{\alpha_m}^{\alpha_m + \delta_m} \cos n\omega t d(\omega t) - \int_{\pi + \alpha_m}^{\pi + \alpha_m + \delta_m} \cos n\omega t d(\omega t) \right] \quad \text{---->(20)}$$

$$= \frac{2V_s}{n\pi} \sin \frac{n\delta_m}{2} \left[\text{Sinn}(\alpha_m + \delta_m/2) - \text{Sinn}(\pi + \alpha_m + \delta_m/2) \right] \quad \text{----->(21)}$$

The coefficient Bn in the general equation of Fourier coefficient can be found by adding the effect of all pulses

$$B_n = \sum_{m=1}^P \frac{2V_s}{n\pi} \sin \frac{n\delta_m}{2} \left[\text{Sinn}(\alpha_m + \delta_m/2) - \text{Sinn}(\pi + \alpha_m + \delta_m/2) \right] \quad \text{---->(22)}$$

For n=1, 3, 5,.....

The pulse width and the pulse location can be determined as:

If the period of carrier frequency per half period of reference wave is represented as k, and the period for reference sine wave as T, and m is the ratio of the peak of carrier wave to that of the peak-to-peak of reference wave (i.e modulation index)

$$t_i = \left(\frac{T}{2k} \right) (i + 0.5) \quad i=0, 1, 2, \dots \quad \text{---->(23)}$$

And the pulse width δ_m is given as

$$\delta_m = \left(\frac{T}{2k} \right) [1 + (-1)^i m \sin \omega t_i] \quad \text{---->(24)}$$

$$B_n = \frac{4}{T} \int_0^{T/2} E_{tpi}(\delta(t_i)) \text{Sinn} \omega_0 t dt \quad \text{---->(25)}$$

Substituting for δ_m

$$= \frac{2mE}{k} \sum_{i=0}^{k-1} \sin \omega_0 t_i [\sin n \omega_0 t_i] \quad \text{---->(26)}$$

Based on these equations, the pulse width, its corresponding pulse location and the amplitude can be determined theoretically and tabulated. For instance, with the value of k = 30, m= 0.5; that is there are thirty pulses per half cycle with 0.5 modulation index. The pulse location(ti) and the corresponding width(δ_m) can be tabulated. This design was implemented with software simulation and the results show that the concept was correct.

III. CONCLUSION

The increasing use of PWM inverter-fed induction motors' application necessitated in-depth analysis for optimum performance. This paper has analysed the main parameters in a pulse width modulated inverter design. The mathematical models were derived and numerical values obtained specifically for a 0.5 Hp induction motor. The expressions for line current, pulse width and its location were determined analytically. The

circuit components designed for the specific application which include resistance and inductance as well as switching frequency were presented. The use of filter is however recommended to reduce the high value of harmonic frequency in the circuit. The results validate the simulation and implementation results earlier obtained. The design methodology can be employed as a guide for industrial and general applications.

REFERENCES

- [1]. Pal, V.K. and Singh, S. (2020). Design of Sinusoidal Pulse Width Modulation 3 Phase Bridge Inverter. International Research Journal of Engineering and Technology (IRJET) e-ISSN: 2395-0056. Vol: 07 Issue: 07. www.irjet.net
- [2]. Agarwal, M.A. and Joshi, D.K. (2018) Performance Analysis of a Three Phase Induction Motor Fed by Three Phase PWM VSI Using Variable Modulation Index. International Journal of Advance Research and Innovation 169 IJARI. Volume 6, Issue 3 (2018), 169-171 ISSN 2347-3258.
- [3]. Rahman, A. Rahman, M. and Islam, R. (2017) Performance Analysis of Three Phase Inverters with Different Types of PWM Techniques. 2nd International Conference on Electrical & Electronic Engineering (ICEEE), 27-29 December 2017, RUET, Rajshahi, Bangladesh 978-1-5386-3341-0/17/\$31.00 ©2017 IEEE.
- [4]. Muhammed Alaudeen Ashiq, M., Jessi Sahaya Shanthi, L. (2021). Simulation of Electric Vehicle Driven by PWM Inverter Fed Induction Machine. In: Komanapalli, V.L.N., Sivakumaran, N., Hampannavar, S. (eds) Advances in Automation, Signal Processing, Instrumentation, and Control. Lecture Notes in Electrical Engineering, vol 700. Springer, Singapore. https://doi.org/10.1007/978-981-15-8221-9_246.
- [5]. Alzuabid, O.H.A. (2022) Study and implementation sinusoidal PWM inverter fed 3-phase induction motor Int. J. Nonlinear Anal. Appl. 13 (2022) 1, 3293-3303 ISSN: 2008-6822 (electronic) <http://dx.doi.org/10.22075/ijnaa.2022.6082>.
- [6]. Ogunyemi, J. (2013). Electronics Simulation of Phase Shift Circuit for Three-Phase Pulse Width Modulated (PWM) Inverter. International Journal of Engineering Research & Technology (IJERT). Vol. 2 Issue 12, November-2013.
- [7]. Ogunyemi, J. Bitrus, I. & Mathew T. O. (2019) Design and Implementation of Triangular Waveform and Pulse Generators for Three-phase PWM Inverter Feeding Induction Motor. Iconic Research and Engineering Journals. Vol. 3 Issue 6. Paper ID: 1701847.
- [8]. Kadam, A. and Shaikh, A.N. (2014) Simulation & Implementation Of Three Phase Induction Motor On Single Phase By Using PWM Techniques. International Journal of Engineering Research and General Science Volume 2, Issue 6, October-November, 2014 ISSN 2091-2730 93 www.ijergs.org.
- [9]. International IOR rectifier (2007) HV Floating MOS-Gate Driver ICs. Pp 001-0030
- [10]. Ojha, P. K. et al, (2020) Speed Regulation and Control of Inverter Fed Induction Motor Drives Using Controllers (PI, PID). Current Journal of Applied Science and Technology 39(9): 7-14, 2020; Article no. CJA5T.56515. ISSN: 2457-1024
- [11]. Shera, H.A. et al (2017) Theoretical and experimental analysis of inverter fed induction motor system under DC link capacitor failure. Journal of King Saud University – Engineering Sciences. www.ksu.edu.
- [12]. Murphi, J.M.D & Turnbull F.G. (1998) "Power electronic control of AC motors" Pergamon Press, 1st edition, (1988).
- [13]. V3.03 (2005) A Technical Guide to Building Fighting Robot: Speed Controller. V3.03 5-Oct-2005. <http://robots.freehostia.com/SpeedControl/SpeedControllersBody.html>.